Conformationally Selective Binding of Nucleotide Analogues to *Escherichia coli* RecA: A Ligand-Based Analysis of the RecA ATP Binding Site†

Tim J. Wigle, Andrew M. Lee, and Scott F. Singleton*

School of Pharmacy, Division of Medicinal Chemistry and Natural Products, University of North Carolina, CB #7360, Chapel Hill, North Carolina 27599-7360

Received November 9, 2005; Revised Manuscript Received February 7, 2006

ABSTRACT: The roles of the RecA protein in the survival of bacteria and the evolution of resistance to antibiotics make it an attractive target for inhibition by small molecules. The activity of RecA is dependent on the formation of a nucleoprotein filament on single-stranded DNA that hydrolyzes ATP. We probed the nucleotide binding site of the active RecA protein using modified nucleotide triphosphates to discern key structural elements of the nucleotide and of the binding site that result in the activation of RecA for NTP hydrolysis. Our results show that the RecA-catalyzed hydrolysis of a given nucleotide triphosphate or analogue thereof is exquisitely sensitive to certain structural elements of both the base and ribose moieties. Furthermore, our ligand-based approach to probing the RecA ATP binding site indicated that the binding of nucleotides by RecA was found to be conformationally selective. Using a binding screen that can be readily adapted to high-throughput techniques, we were able to segregate nucleotides that interact with RecA into two classes: (1) NTPs that preferentially bind the active nucleoprotein filament conformation and either serve as substrates for or competitively inhibit hydrolysis and (2) nonsubstrate NTPs that preferentially bind the inactive RecA conformation and facilitate dissociation of the RecA−DNA species. These results are discussed in the context of a recent structural model for the active RecA nucleoprotein filament and provide us with important information for the design of potent, conformationally selective modulators of RecA activities.

Antibiotic resistance in pathogenic bacteria is a growing problem that has a tremendous socioeconomic impact worldwide. The mechanisms leading to the development and transmission of antibiotic resistance are not fully understood, but the bacterial RecA protein has been identified as a likely player in this phenomenon. RecA facilitates the development of antibiotic resistance via its roles in stress-induced DNA repair (*1*−*3*) and the horizontal transfer of genes between organisms (*4*, *5*). The functions of RecA require the formation of a nucleoprotein filament composed of RecA, ssDNA,[1] and ATP. This activated filament is responsible for induction of the SOS response to genomic damage by stimulation of LexA repressor autoproteolysis, and it also directly participates in recombinational DNA repair (*6*, *7*). Because of these vital roles within prokaryotes, RecA remains an attractive target for mechanistic and pharmacologic study (*8*, *9*).

Investigation of the structure of RecA using EM directly demonstrated two structurally distinct RecA−ssDNA filaments (*10*, *11*). A collapsed filament forms on ssDNA in the absence of the nucleotide cofactor or in the presence of ADP, while an extended filament is formed when ATP or its slowly hydrolyzed analogue, ATPγS, is present. The collapsed filament represents the inactive conformation of RecA with a relatively low affinity for ssDNA, while the extended filament represents an active conformation of RecA that binds ssDNA more tightly (*12*, *13*). The interconversion from inactive to active nucleoprotein filament does not simply occur via direct conformational isomerization upon binding of ATP (*14*−*16*). Rather, this conversion consists of ATP binding to the inactive filament, causing it to dissociate from DNA, followed by reassociation of the ATP-bound monomers with the ssDNA which forms the activated RecA nucleoprotein filament (*16*). Other nucleotides, particularly ADP, bind and stabilize the inactive conformation and cause the release of RecA from DNA without inducing the conformational change leading to the activated state (*13*, *16*). The design of nucleotide analogues capable of differentiating the active and inactive conformations of RecA is an ongoing research interest in our laboratory (*9*). The discovery of such small molecules, which has implications for the development of RecA-specific ligands capable of either (1) preventing RecA conformational activation by selectively binding the inactive conformation or (2) competing with ATP by selectively binding the active conformation, would be facilitated by an understanding of the RecA structural determinants of conformationally selective ligand binding.

† This work was supported by a grant from the National Institutes of Health (GM58114) to S.F.S.

* To whom correspondence should be addressed. Telephone: (919) 966-7954. Fax: (919) 966-0204. E-mail: sfs@unc.edu.

[1] Abbreviations: ATPγS, adenosine 5′-*O*-(thiotriphosphate); EM, electron microscopy; MANT-ATP, 2′(3′)-*O*-(*N*-methylanthraniloyl)-adenosine 5′-*O*-triphosphate; MESG, 7-methylthioguanosine (2-amino-6-mercapto-7-methylpurine riboside); NPF, nucleoprotein filament; NDP, nucleoside 5′-*O*-diphosphate; NTP, nucleoside 5′-*O*-triphosphate; nts, nucleotides; PNP, purine nucleoside phosphorylase; ssDNA, single-stranded DNA.

10.1021/bi052298h CCC: $33.50
Published on Web 03/21/2006

A variety of experimental approaches have demonstrated selectivity in the binding and hydrolysis of NTPs by the active RecA filament (*13*, *17*−*22*). Although a wealth of information is available about the structure of the RecA protein itself (*6*, *23*, *24*), few insights into atomic details of the basis for NTP selectivity have been provided by the crystal structures. In part, this dearth of information arises from the fact that the adenosine moiety of RecA resides within a wide, shallow, and solvent-exposed cleft on the surface of RecA (*9*). The lone residue making a potentially base-specific contact with an adenosine nucleotide is Asp100, and Bryant and co-workers have suggested that the specificity of RecA for ATP was due in part to a hydrogen bond between the Asp100 carboxylate and the exocyclic 6-amino group of ATP (*25*). Our own recent observations, however, suggest that the negatively charged side chain of Asp100 creates an electrostatic potential pattern that regulates the transduction of ATP binding into conformational activation for DNA binding and higher-order processing and, as a consequence, discriminates against GTP (and ITP) binding and usage (A. M. Lee and S. F. Singleton, in press). Unfortunately, a high-resolution structure of the active conformation of RecA has not been reported, and the key structural determinants of the dynamic equilibrium between inactive and active RecA filaments remain elusive.

To date, the crystal structures have not provided specific molecular insight into the binding selectivity of the ATP site in an activated RecA filament. Therefore, more indirect methods are needed to characterize the structural features of the site. In this study, we probed the nucleotide binding site of RecA using a systematic, ligand-based approach involving a total of 28 prospective ligands comprising both canonical NTPs and 19 synthetic analogues never previously tested with RecA. Using three rapid screening assays, we characterized binding of the nucleotide to either the active RecA filament, the inactive RecA filament, or both. The data clearly demonstrate that the nucleotides can be segregated into two groups based on mutually exclusive activities in the three assays: (1) nucleotides that preferentially bind the active NPF conformation and either serve as substrates for or competitively inhibit hydrolysis and (2) nonsubstrate NTPs that preferentially bind the inactive RecA conformation and facilitate dissociation of the RecA−ssDNA species. The observations are consistent with the recently reported pseudo-atomic model of the active state of RecA based on an 18 Å EM reconstruction of the active NPF (*11*). In this model, the ATP binding site is located between adjacent RecAs such that an ATP interacts with the P-loop and several key residues of one RecA subunit, and a neighboring RecA monomer completes the binding site by enveloping the adenine moiety. These results have important implications not only for the elucidation of important structural details of the nucleotide binding site of the active RecA filament but also for the design of specific, potent, and conformationally selective ligands for modulating RecA activities.

EXPERIMENTAL PROCEDURES

Materials. The *Escherichia coli* RecA protein was purified as described previously (*26*) to ≥97% homogeneity and stored in aqueous buffer [25 mM Tris-HCl (pH 7.5), 1 mM DTT, and 5% glycerol] at −80 °C. The protein concentration was determined using a monomer extinction coefficient of 2.2×10^4 M^{-1} cm^{-1} at 280 nm (*27*). ATP, dATP, GTP, dGTP, ITP, dITP, CTP, dCTP, UTP, TTP, and 8-bromo-ATP were purchased from Sigma Aldrich (St. Louis, MO) as their sodium salts at the highest level of purity possible (see Figure 1 for NTP structures). Ara-ATP, 2′-OMe-ATP, 3′-OMe-ATP, 2′-NH_2-ATP, 2′-F-ATP, 2-NH_2-ATP, 6-Cl-PTP, 2′-OMe-ATP, 5-Me-UTP, 5-Me-CTP, 5-propynyl-dUTP, and O^6-Me-GTP were purchased from TriLink Biotechnologies (San Diego, CA) as their sodium salts. MANT-ATP, N^6-benzyl-ATP, and N^6-phenyl-ATP were purchased from AXXORA (San Diego, CA) as their sodium salts. N^6-(1-Naphthyl)-ATP was synthesized as described previously (*9*). The EnzChek phosphate assay kit, which includes purine nucleoside phosphorylase enyzme (PNP) and 7-methylthioguanosine substrate (MESG), was purchased from Invitrogen (Carlsbad, CA). Poly(dT) ssDNA (average length of 319 nucleotides) was purchased from Amersham Biosciences (Piscataway, NJ). Desalted biotin-$(dT)_{36}$ was purchased from Sigma Genosys (The Woodlands, TX) and used without further purification. Streptavidin paramagnetic particles (SA-PMP) were from Promega. Clear 96-well flat-bottom microplates were purchased from Evergreen Scientific (Los Angeles, CA).

Nucleotide Triphosphate Hydrolysis Assays. The hydrolysis of NTPs by RecA was assessed using a published enzyme-coupled continuous spectrophotometric assay for inorganic phosphate release (*28*). Reactions (final volume of 100 μL) were initiated in a 96-well microplate by adding a preincubated solution containing 0.5 μM RecA, 10 mM $Mg(OAc)_2$, 1 mM DTT, 15 μM-nts poly(dT), 0.3 mM MESG, and 1 unit/mL PNP in 25 mM Tris-HOAc (pH 7.5) at 25 °C with 5% (v/v) glycerol to various concentrations of nucleotide triphosphate (from 0 to 1000 μM). The A_{360} was monitored every 30 s in the microplate reader at 37 °C for 30 min using a Perkin-Elmer HTS 7000+ bioassay reader with a 360 ± 5 nm band-pass filter. The initial, steady-state reaction velocity (v°_{obs}; in micromolar per minute) for each NTP was calculated from the change in absorbance as a function of time ($\partial A/\partial t$) using a $\Delta\epsilon_{360}$ of 6.0×10^{-4} μM^{-1} as measured in the microplate reader. Each set of data, corresponding to a range of NTP concentrations, was analyzed using a Michaelis−Menten equation modified for substrate cooperativity as described previously (*29*, *30*):

$$v^\circ_{obs} = k_{cat} R_0 \frac{[NTP]^3}{[NTP]^3 + S_{0.5}{}^3} \quad (1)$$

where R_0 is the total concentration of RecA and $S_{0.5}$ is the NTP concentration when the velocity is half of its maximum value.

Inhibition of ATPase Activity by Selected Nucleotides. A solution containing 0.5 μM RecA, 100 μM nucleotide, 10 mM $Mg(OAc)_2$, 1 mM DTT, 0.3 mM MESG, and 1 unit/mL PNP in 25 mM Tris-HOAc (pH 7.5) at 25 °C was mixed with 5% (v/v) glycerol for 5 min at 37 °C. The ATPase reactions were initiated by the addition of a solution containing ATP and poly(dT) (final concentrations of 500 μM and 1.5 μM-nts, respectively) to achieve a final reaction volume of 600 μL. The change in A_{360} was recorded for 30 min at 37 °C in a Perkin-Elmer Lambda 20 UV−vis

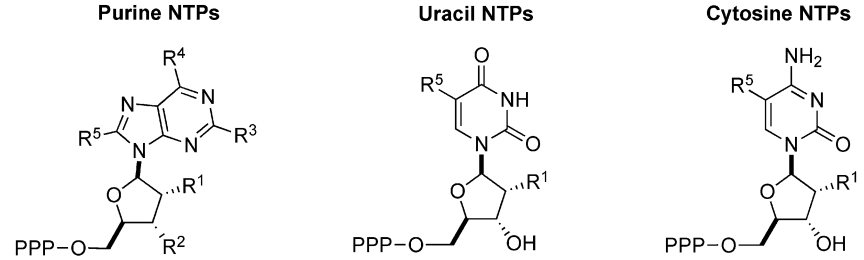

Entry	Nucleoside	R^1	R^2	R^3	R^4	R^5	Abbreviation
			ATP Analogs				
1	araadenosine	OH[a]	OH	H	NH_2	H	Ara-ATP
2	2′-*O*-methyladenosine	OMe	OH	H	NH_2	H	2′-OMe-ATP
3	3′-*O*-methyladenosine	OH	OMe	H	NH_2	H	3′-OMe-ATP
4	2′-aminoadenosine	NH_2	OH	H	NH_2	H	2′-NH_2-ATP
5	2′-fluoroadenosine	F	OH	H	NH_2	H	2′-F-ATP
6	6-chloropurineriboside	OH	OH	H	Cl	H	6-Cl-PTP
7	2,6-diaminopurineriboside	OH	OH	NH_2	NH_2	H	2-NH_2-ATP
8	8-bromoadenosine	OH	OH	H	NH_2	Br	8-Br-ATP
9	N^6-phenyladenosine	OH	OH	H	NHPh	H	N^6-Phe-ATP
10	N^6-benzyladenosine	OH	OH	H	$NHCH_2Ph$	H	N^6-Bn-ATP
11	N^6-1-naphthyladenosine	OH	OH	H	NH(1-Naphthyl)	H	N^6-Np-ATP
12	O^6-methylguanosine	OH	OH	NH_2	OMe	H	O^6-Me-GTP
			CTP Analogs				
13	5-methylcytidine	OH	–	–	–	Me	5-Me-CTP
			UTP Analogs				
14	2′-*O*-methyluridine	OMe	–	–	–	H	2′-OMe-UTP
15	5-methyluridine	OH	–	–	–	Me	5-Me-UTP
16	5-propynyl-2′-deoxyuridine	OH	–	–	–	$C{\equiv}CCH_3$	5-propynyl-dUTP

FIGURE 1: Non-natural nucleotide analogues used in this work. The abbreviation "PPP" indicates that a triphosphate moiety ($P_3O_7^{4-}$) is appended at the 5′-O-position of each depicted nucleotide. The stereochemistry of the first OH in the R^1 column is the opposite of that of the representative purine NTP shown.

spectrophotometer with a thermojacketed six-cell changer regulated by a Peltier temperature control system. The v_{obs}° values were determined as described above using a $\Delta\epsilon_{360}$ of 1.1×10^4 M^{-1} cm^{-1}, and the percent inhibition was calculated relative to the velocity in the absence of any added inhibitor.

Assessment of ATPase Inhibition and Determination of Inhibition Constants (K_{ic}). ATPase kinetic measurements were carried out as previously described (*31*, *32*) with modifications for microplate measurements. Briefly, reactions (volume of 100 μL) were initiated in a microplate by adding 15 μM-nts poly(dT) to a solution of nucleotide (0−1000 μM), 0.5 μM RecA, 10 mM $Mg(OAc)_2$, 3 mM ATP, 2 mM NADH, 2.3 mM phosphoenolpyruvate, 5 units/mL pyruvate kinase, and 5 units/mL lactic dehydrogenase. The decrease in A_{380} was recorded as a function of time for 30 min at 37 °C in a Perkin-Elmer HTS7000+ bioassay reader using a 380 ± 10 nm band-pass filter. The $S_{0.5}^{app}$ values were measured as described above in the presence of different concentrations of inhibitor. The K_{ic} values were determined by linear regression analysis of plots of $S_{0.5}^{app}$ as a function of inhibitor concentration.

Inhibition of ssDNA Binding by Selected Nucleotides. RecA (4 μM) was incubated at 37 °C for 20 min with 100 μM nucleotide, 18 μM-nts biotin-$(dT)_{36}$, 2 μM ATPγS, 60 mM NaCl, and 1 mM DTT in 1× assay buffer [25 mM Tris-HOAc (pH 7.5) at 25 °C, 5% (v/v) glycerol, and 10 mM $Mg(OAc)_2$] in a total volume of 50 μL. In optimization trials, the inclusion of NaCl and substoichiometric amounts of ATPγS were found to maximize the signal-to-background ratio for the assay, where the signal is defined as the amount of RecA released in the presence of 100 μM ADP and the background is defined as the amount of RecA released in the absence of any additional nucleotide (data not shown). SA-PMP beads were washed three times with 1× assay buffer by resuspension in buffer followed by pelleting with a magnet and removal of the supernatant. The entire 50 μL reaction volume was added to the washed SA-PMP beads and was mixed thoroughly to ensure coating of the beads with the reaction mixture. The reaction mixtures with beads were incubated for 20 min at 37 °C in an Eppendorf Thermomixer R microplate incubator. After the incubation period, the SA-PMP beads were pulled down with a microplate magnet and 10 μL of the supernatant was removed to a second microplate. To this supernatant was added 200 μL of Protein Assay Reagent (Bio-Rad), and the absorbance of the resulting solution was measured in the microplate reader using a 595 ± 25 nm band-pass filter. The A_{595} value was converted to RecA concentration by comparison with a RecA standard curve to quantify the RecA remaining in the supernatant.

Assessment of Apparent RecA−ssDNA Dissociation Induced by Nucleotides. RecA dissociation, induced by the various nucleotides, was assessed as described above over a fixed nucleotide concentration range (0−1000 μM). The apparent dissociation constants (K_d^{app}) were determined by nonlinear least-squares analysis of the resulting titration isotherms using the following equation:

$$A_{595} = A_{min} + (A_{max} - A_{min})\frac{[NTP]}{[NTP] + K_d^{app}} \qquad (2)$$

where A_{min} and A_{max} are the minimum and maximum absorbance values, respectively.

Molecular Model Building for the Active Filament Conformation. The all-atom model of the active RecA filament was constructed by superimposing the C_α backbone of the Xing and Bell crystal structure [PDB entry 1XMV (*33*)] onto the C_α backbone of two adjacent RecA filament subunits of the Egelman laboratory electron microscopy model of the active filament [PDB entry 1N03 (*11*)]. A simple minimization of the superimposed, all-atom structure was then performed using Insight II (Accelrys) to relieve steric clashes between residues due to adjustments in their position made during alignment.

RESULTS

The purpose of our studies was to probe the specificity of the ATPase active site of RecA by characterizing the ability of various nucleotides and their analogues to bind and serve as substrates for RecA-catalyzed hydrolysis. As a first step, NTPs were first assayed for activity with RecA in a DNA-dependent NTPase assay. Those NTPs that could be hydrolyzed were then fully characterized with respect to the steady-state kinetic constants, k_{cat} and $S_{0.5}$. If a given NTP was not hydrolyzed by RecA at a concentration of ≤ 250 μM, it was assayed for (1) inhibition of ATPase activity and (2) inhibition of RecA NPF formation. As described below, the latter two assays were used to segregate nonsubstrate NTPs into groups of nucleotides that either bind to the active RecA nucleoprotein filament, prevent RecA activation and filament formation, or have neither of these two effects.

Steady-State Hydrolysis of Modified NTPs by the RecA Nucleoprotein Filament. Our initial work explored the extent to which modification of the nucleotide base or ribose functional groups affected the ability of RecA to hydrolyze NTPs. We chose to examine 20 analogues of the eight canonical ribo- and 2′-deoxyribonucleotides that span a range of steric and electronic modifications on the purine and pyrimidine heterocycles and the 2′ and 3′ positions of the ribose ring (Figure 1).

Normally, active nucleoprotein filament formation occurs when RecA is simultaneously bound to ATP and ssDNA and results in ATP hydrolysis. Hence, ssDNA-dependent NTP hydrolysis serves as a useful indicator that a NTP promotes active filament formation in vitro. We monitored the steady-state kinetics of the poly(dT)-dependent NTPase activity of RecA using a known enzyme-coupled continuous spectrophotometric assay for inorganic phosphate (*28*). Quantitative control experiments to evaluate the potential influence of the substrates or products of the coupled reaction on the steady-state kinetic parameters for ATP turnover by RecA revealed no measurable effects on V_{max}, $S_{0.5}$ for ATP, or K_d^{app} for poly(dT) binding. Further control experiments for each NTP confirmed that the hydrolysis activity was poly(dT)-dependent and that the enzyme of the coupling system, PNP, was not affected by the NTP (data not shown). For each of the 28 NTPs, the initial steady-state rates of P_i formation were plotted as a function of the total NTP concentration, and nonlinear least-squares curve fitting using eq 3 yielded the rate constant for catalytic turnover, k_{cat}, and the NTP concentration required for half-maximal velocity, $S_{0.5}$ (Table 1). To facilitate comparisons among the NTPs, specificity constants relative to that of ATP were also tabulated. Considering the data for the 20 NTPs that were hydrolyzed at a measurable rate, it is clear that the $S_{0.5}$ values span a range (>40-fold) much wider than that of the k_{cat} values (2-fold). Interestingly, nine NTPs were not hydrolyzed under the experimental conditions, even at concentrations as high as 1 mM (20-fold greater than $S_{0.5}$ for ATP). The structure−activity relationships summarizing the key structural elements that influence the hydrolysis of purine- or pyrimidine-based NTP analogues are illustrated in Figure 2.

Table 1: Kinetics of NTP Hydrolysis by the RecA Protein[a]

nucleotide	k_{cat} (min^{-1})	$S_{0.5}$ (μM)	$(k_{cat}/S_{0.5})_{rel}$
ATP	20 ± 1	50 ± 2	1.0
dATP	22 ± 1	39 ± 1	1.4
Ara-ATP	22 ± 1	86 ± 8	0.65
2′-OMe-ATP	nd[b]	>1000	−
3′-OMe-ATP	19 ± 1	56 ± 8	0.82
2′-NH_2-ATP	27 ± 2	110 ± 20	0.62
2′-F-ATP	15 ± 1	110 ± 30	0.33
6-Cl-PTP	17 ± 1	99 ± 8	0.42
2-NH_2-ATP	27 ± 1	54 ± 5	1.2
8-Br-ATP	18 ± 1	140 ± 10	0.33
N^6-Ph-ATP	24 ± 3	49 ± 6	1.2
N^6-Bn-ATP	33 ± 1	280 ± 30	0.29
N^6-Np-ATP	nd[b]	>1000	−
GTP	15 ± 1	1400 ± 200	0.03
dGTP	21 ± 1	620 ± 30	0.08
O^6-Me-GTP	nd[b]	>1000	−
ITP	22 ± 1	240 ± 10	0.23
dITP	21 ± 1	600 ± 20	0.09
CTP	21 ± 1	290 ± 20	0.09
dCTP	25 ± 1	200 ± 10	0.32
5-Me-CTP	nd[b]	>1000	−
UTP	25 ± 1	350 ± 40	0.09
dUTP	25 ± 1	110 ± 30	0.58
5-propynyl-dUTP	nd[b]	>1000	−
5-Me-UTP	nd[b]	>1000	−
TTP	nd[b]	>1000	−
2′-OMe-UTP	nd[b]	>1000	−

[a] Kinetics of ATP hydrolysis were measured using the MESG/PNP system to detect release of free phosphate. Each kinetic parameter was determined in triplicate, and the error shown is the standard deviation of three trials. [b] Hydrolysis was not detected at concentrations of 1000 μM.

For the eight canonical (r,d)NTPs, the data obtained using the PNP-coupled system recapitulated previously reported conclusions (*13*). Specifically, the order of decreasing $k_{cat}/S_{0.5}$ was as follows: (r,d)ATP > UTP > (r,d)CTP > (r,d)GTP ≫ TTP. While ATP is the preferred substrate, it is not necessarily the purine ring that leads to the selectivity. GTP and ITP, both of which are purine nucleotides, were able to stimulate only RecA activation with $S_{0.5}$ values of 240 and 1400 μM, respectively. ITP and GTP have a carbonyl group at position C6 in lieu of the exocyclic amine of ATP, and this appears to attenuate the ability of those nucleotides to activate RecA. Previous studies by the Bryant laboratory have suggested that the specificity of RecA for ATP was due in part to a hydrogen bond between the Asp100 carboxylate and the exocyclic 6-amino group of ATP (*25*). We have observed that the specificity for ATP over GTP and ITP does not appear to be entirely related to hydrogen bonding as 6-Cl-PTP, which is unable to hydrogen bond with the D100 position, is an efficient substrate of RecA.

Several aspects of the kinetic results (Figure 2) are not readily explained by examination of the open ATP binding site observed in crystal structures of RecA bound to different nucleotides (*33*−*35*). For example, ATP modifications such

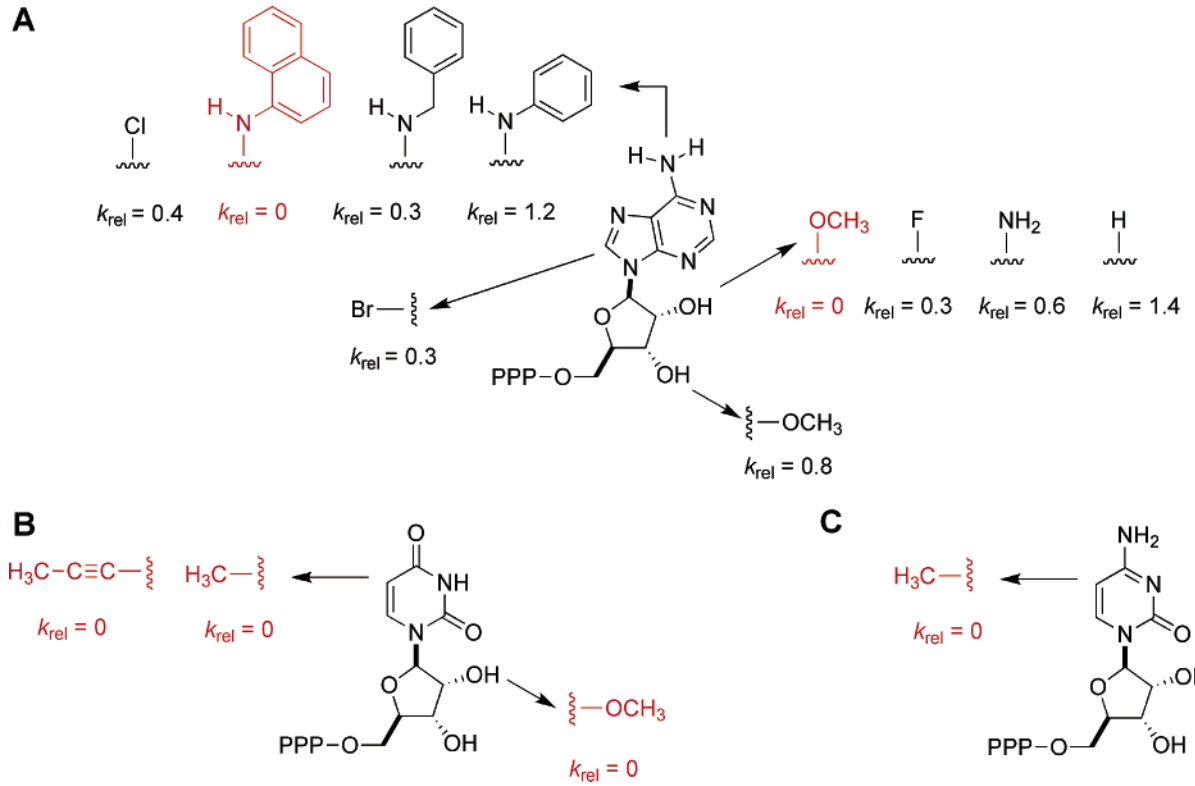

FIGURE 2: Analysis of structure−activity relationships for RecA-catalyzed NTP hydrolysis of ATP analogues (A), UTP analogues (B), and CTP analogues (C). The kinetic constants are compared to that of ATP using the relation $k_{rel} = (k_{cat}/S_{0.5})_{NTP}/(k_{cat}/S_{0.5})_{ATP}$ (see Table 1). Modifications abrogating all RecA activity are colored red.

as 2′-F or 2′-NH_2, which change the electronic character but not the steric size of the 2′ position, were tolerated well by RecA. However, the slight steric increase arising from the replacement of the 2′-OH group with a 2′-OMe group abolished the hydrolytic activity of RecA. Hydrogen bonding by the C2′ substituent was not a requirement for RecA's NTPase activity as dATP and Ara-ATP resulted in hydrolysis kinetics essentially identical to those of ATP. Remarkably, the effect of the OH → OMe change was restricted to C2′: when the 3′-OH group was replaced with a 3′-OMe group, there was no substantial change in the kinetic parameters of NTP hydrolysis. The inability of RecA to hydrolyze NTPs modified with groups larger than a hydroxyl at the C2′ position also extended to pyrimidines as 2′-OMe-UTP was not turned over by RecA. Moreover, MANT-ATP, which was utilized as a mixture of regioisomers with an aromatic substituent at either the ribose 2′- or 3′-hydroxyl, was not a substrate for RecA NTPase activity.

The substitution of a methyl group for the hydrogen atom at the C5 position of pyrimidine NTPs also eliminated the ability of RecA to utilize such nucleotides as substrates. Indeed, the natural nucleotide TTP and the C5-substituted nucleotides 5-Me-UTP, 5-Me-CTP, and 5-propynyl-dUTP were not RecA substrates. Presumably, the 5-methyl groups of such pyrimidine NTPs occupy an area of space corresponding to the likely positions of prospective substituents at the N7 and C8 positions of a purine NTP. The idea that a similar effect would be produced by adding a CH_3-sized substituent at N7 or C8 of ATP was only partially confirmed: we observed 8-Br-ATP to be a modest substrate of RecA NTPase activity.

Contrary to the tight tolerances on the size of substituents at C2′ of all NTPs and at C5 of pyrimidine NTPs, RecA was able to accommodate aromatic modifications at the N^6 position of adenosine. A phenyl ring appended to the N^6-amino group had essentially no effect on hydrolysis, while a benzyl group at the N^6 position, which has more rotational degrees of freedom than the phenyl substituent, increased k_{cat} significantly but also increased $S_{0.5}$. A naphthyl substitution at the N^6 position yielded an adenosine nucleotide that was not hydrolyzed by RecA.

Although the RecA active site for ATP hydrolysis can accommodate sterically demanding substituents as large as a benzyl group, replacement of the exocylic NH_2 group with an OMe group at position 6 of a purine to produce O^6-Me-GTP abrogated ATP hydrolysis. Three trivial structural rationales for this observation can be ruled out by internal controls. First, the presence of an exocyclic NH_2 group at C2 of O^6-Me-GTP likely has little influence on its resistance to hydrolysis by RecA because the same functional group in the context of the adenine heterocycle (2-NH_2-ATP) had only modest effects on the kinetic parameters. A second possible explanation for the 6-NH_2 to 6-OMe effect is the removal of a hydrogen bond donor. However, this possibility is ruled out as replacement of the NH_2 group with a Cl atom (6-Cl-PTP) had an only modest effect on RecA's NTPase activity. Likewise, purine riboside 5′-*O*-triphosphate, which has no exocyclic functional groups, has been shown to be a substrate for RecA-catalyzed hydrolysis (*20*). Finally, the potential impact of a syn glycosidic torsional preference for unbound O^6-Me-GTP (*36*) is minimized by the observation that 8-Br-ATP which has a similar syn preference (*37*, *38*) was hydrolyzed in a manner similar to that of ATP.

The molecular determinants of attenuation of the DNA-dependent NTPase activity of RecA can be summarized as follows. Substitution at the C2′ position of the ribose ring

with groups larger than a hydroxyl moiety prevented both purine- and pyrimidine-based NTPs from acting as substrates for RecA NTPase activity. Replacement of the N^6-amino group of the adenine ring with aromatic groups larger than benzyl disrupted the ability of RecA to use the NTP as a substrate. Likewise, addition of a methyl group or propynyl group at the C5 position of pyrimidine NTPs produced the same effect.

A Rapid Screen for Active NPF Binding by Nonsubstrate NTPs. Although we were able to determine the kinetic parameters k_{cat} and $S_{0.5}$ for hydrolysis of 19 NTPs, the interpretation of the negative results for the other nine NTPs is complicated by the nature of the complex series of events leading to an activated NPF state and subsequent hydrolysis (*16*, *39*, *40*). In particular, we could not determine whether the nonsubstrate NTPs were binding to the RecA ATP binding site without being turned over. To investigate this possibility, we assessed the inhibition of RecA poly(dT)-dependent ATPase activity by nonsubstrate nucleotides. Under the conditions of this assay, which includes excess ATP (0.5 mM), RecA maintains its active conformation during steady-state turnover of ATP. To impact the rate of ATP hydrolysis by RecA, a general ligand must be able to bind the active nucleoprotein filament and a NTP must be able to compete with 0.5 mM ATP for its binding site on RecA.

In conjunction with our previous work which explored potential inhibitors of RecA activities (*9*), we desired a rapid, high-throughput screening compatible assay for characterizing the influence of select small molecules on the poly(dT)-dependent ATPase activity of RecA. To optimize a single-point screen (one ATP concentration and one inhibitor concentration) for identifying nonsubstrate nucleotides that bind the active NPF, we measured the inhibition constants, K_{ic}, for the ATP-competitive inhibition of ATP turnover and compared the K_{ic} values to a single point of relative ATPase inhibition. The analysis included data for six of the nine nonsubstrate NTPs and ADP, which is a known inhibitor (*17*, *41*−*43*), and the optimal conditions were found to include 100 μM nucleotide inhibitor and 500 μM ATP. The use of the single-point screening assay was validated by a correlation plot (Figure 3A), suggesting that a single ATPase measurement at 100 μM nucleotide is sufficient to characterize rapidly the inhibitory properties of a particular nucleotide.

Nonsubstrate NTPs Are Low-Affinity Binders of the Active NPF. Interestingly, none of the nonsubstrate NTPs competitively inhibited RecA ATPase activity >10% with the exception of MANT-ATP. At a concentration of 100 μM, MANT-ATP abolished >95% of the ATPase activity in our active NPF binding screen and is consistent with the low K_{ic} value reported here and elsewhere (*44*). A full discussion of the ATP-competitive inhibition of RecA ATPase activity using nucleotide analogues is beyond the scope of this work and will be presented elsewhere.

A Rapid Screen of Inactive NPF Binding by NTPs. The competitive ATPase inhibition analysis provides a method of gauging whether prospective ligands bind to the ATP binding site of RecA during active ATP hydrolysis, and the low extents of ATPase inhibition by the nonsubstrate NTPs indicated that they are not high-affinity binders of the active filament. However, the ATPase inhibition assay does not provide any information about the binding of nucleotides to the inactive NPF. We therefore utilized a method for characterizing the interaction of nucleotides with RecA that does not involve the NTPase activity of the protein.

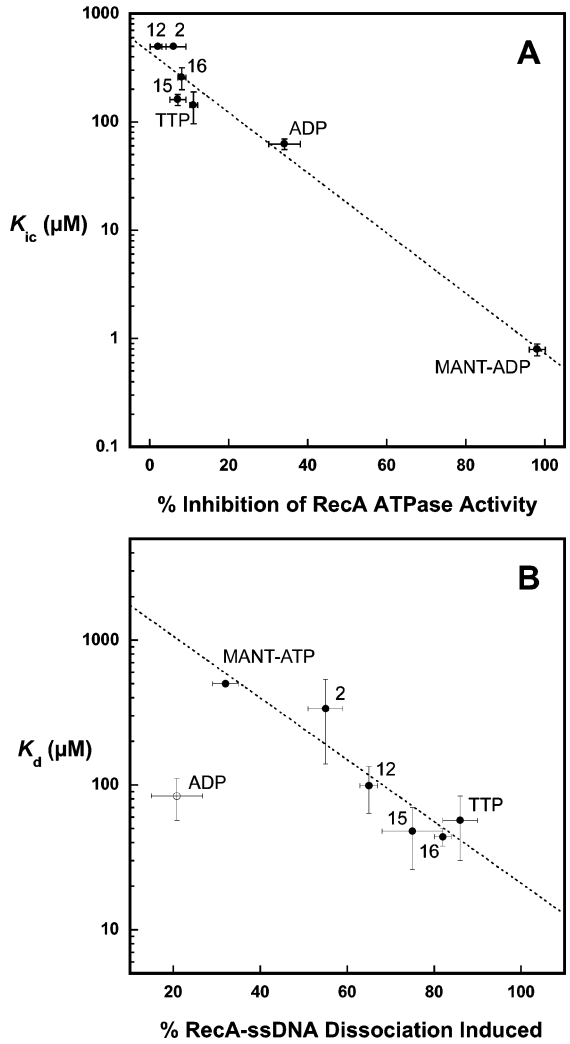

FIGURE 3: Correlation plots for validation of binding screens. (A) The poly(dT)-dependent ATPase K_{ic} of a given nucleotide is plotted as a function of the percent inhibition of RecA poly(dT)-dependent ATPase activity caused by an inhibitor at a single concentration point of 100 μM. The line represents the best fit using the "Exponential" curve fitting function of KaleidaGraph version 4.0 (Synergy Software). Values reported are the averages ± the standard deviation of at least three independent experiments. (B) RecA−ssDNA dissociation constants of nucleotide binding, K_d, of the nucleotides plotted in panel A as determined in the RecA−ssDNA dissociation titration are plotted as a function of their respective percent RecA−ssDNA dissociation induced in our single-point screening assay at an inhibitor concentration of 100 μM. The line shown was fit to the data as described for panel A. The identities of the nucleotides are indicated on the graph, and the numerals correspond to the entry numbers in Figure 1. Values reported are the averages ± the standard deviation of at least three independent experiments. The relationship between potency and efficacy does not hold true for ADP, which binds RecA tightly as indicated by the low K_d value, but the maximum level of dissociation stimulated is much lower than that of the other nucleotides that were studied (see the text for details).

Our laboratory recently developed a high-throughput screening compatible assay to determine the effects of synthetic small molecules on the binding of RecA to ssDNA (*45*). This assay is not competitive with respect to other nucleotides. The assay design takes advantage of two important observations: (1) ADP decreases the stability of

NPFs (*46*), and (2) the addition of ADP to a complex of RecA bound to a 30mer oligonucleotide results in disassembly of the complex and concomitant release of RecA from the DNA (*16*). Hence, for the 96-well microplate assay, $(dT)_{36}$ conjugated to biotin was incubated with RecA and a selected nucleotide at a concentration of 100 μM. The extent to which the selected nucleotide disrupts the binding of RecA to ssDNA is measured by quantifying the amount of RecA displaced into the supernatant after any RecA remaining bound to biotin-$(dT)_{36}$ was pulled down with streptavidin-coated paramagnetic particles.

To ensure that the screen would identify nucleotides that bound RecA and induced its dissociation from ssDNA, we measured the apparent equilibrium dissociation constant for RecA−ADP binding by monitoring the amount of RecA released from (dT_{36})-biotin as a function of ADP concentration. The resulting titration isotherm was fit to a standard equation for a right hyperbola to produce a K_d^{app} of 80 ± 30 μM (data not shown). This value compares favorably to the K_d^{app} of 120 μM reported by Lee and Cox (*15*), verifying that the rapid nucleotide binding assay results are quantitatively related to the extent of RecA−nucleotide binding. As further validation of the assay, we conducted two further control experiments described below.

First, we determined the dissociation constants, K_d^{app}, for binding of nucleotide to RecA and compared these values to a single point of relative displacement of RecA from $(dT)_{36}$-biotin. As described above, the analysis included data for ADP and the same six nonsubstrate NTPs at a concentration of 100 μM in the single-point microplate assay. Considering the data for all of the NTPs, but not for ADP, a correlation was observed between the ability of a nucleotide to facilitate dissociation of a RecA−ssDNA species at a concentration of 100 μM and the K_d^{app} value calculated from a titration of the nucleotide (Figure 3B). It is noteworthy that the data point for ADP fell well off the trend line in the correlation plot (Figure 3B). At a descriptive level, the result for ADP may be attributed to a higher-than-expected potency (i.e., K_d is lower than the correlation predicts), a lower-than-expected efficacy (i.e., the amount of RecA displaced from the NPF is lower than the K_d predicts), or a combination of both. The titration data (not shown) suggest that ADP is less efficacious than expected: the shape of the titration isotherm is indistinguishable from the shapes of those of the nonsubstrate NTPs, while the maximum extent of RecA displacement is lower than that induced by any nonsubstrate NTP. Because RecA·ADP retains the ability to bind ssDNA, albeit with a reduced affinity, the fact that the efficacy of ADP is lower than that predicted by the correlation for this assay may suggest that RecA has a particularly low affinity for ssDNA when bound to one of the nonsubstrate NTPs. This may have important implications if the difference can be generalized to other NTPs.

Second, to establish the robustness of the RecA−ssDNA dissociation assay further, we screened nine pairs of canonical nucleoside di- and triphosphates, both ribo- and 2′-deoxyribonucleotides, for RecA binding. As shown in Figure 4, no differences were detected among the extents of dissociation of the RecA−ssDNA species stimulated by the different di- and triphosphate pairs, with the notable exception of TTP and TDP. These NTPs are uniformly known to be at least moderate substrates for RecA NTPase activity (Table 1). This

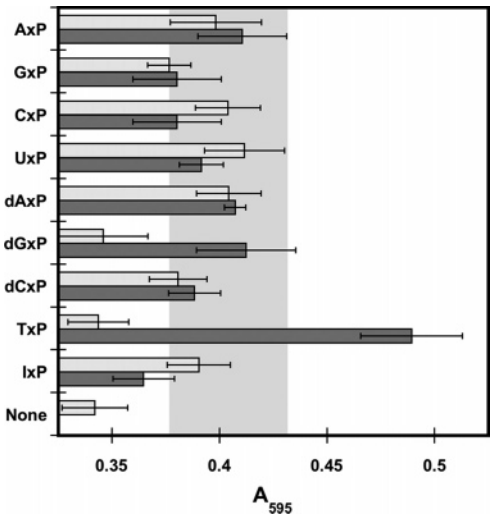

FIGURE 4: Extent of RecA−ssDNA dissociation induced by the presence of various nucleoside diphosphates (gray) and triphosphates (white). Each (r,d)NxP (final concentration of 100 μM) was added to RecA-$(dT)_{36}$ filaments immobilized on SA-PMP as described in Experimental Procedures. The amount of RecA displaced into the supernatant was measured using a Bradford assay (A_{595}). Values reported for each (r,d)NxP are the mean ± standard deviation of at least three independent experiments.

observation is consistent with the fact that the conditions of the DNA displacement screen allow a NTP to be hydrolyzed to the corresponding NDP during the experiment.

The difference in RecA displacement observed with TTP and TDP is significant. TTP is not a RecA substrate under the assay conditions (Table 1), and as such, the displacement we observed is due solely to the presence of TTP. The dramatic extent of RecA displacement from ssDNA by TTP is consistent with the conclusion that TTP binds RecA under these conditions, whereas it could not replace or compete with ATP. In contrast, TDP displaces RecA less effectively than ADP, and the extent of TDP-induced filament dissociation is the same within error as that is observed in the absence of any nucleotide. We conclude that TDP does not bind RecA under these conditions. Taken together, these results suggest that the RecA−ssDNA dissociation screen will be useful for assaying both nonsubstrate nucleotide triphosphates and the nucleoside diphosphate that corresponds to the NTP substrates of RecA NTPase activity.

Nonsubstrate NTPs Bind Preferentially to the Inactive NPF. The nine nucleotides that were not substrates of RecA for hydrolysis at a concentration up to 250 μM were evaluated for potential RecA−ssDNA dissociation using the DNA displacement screening assay. The extents of filament dissociation varied over a wide range, and these values, along with those for the substrate NTPs from Figure 4, were plotted as a function of the relative specificity constant (Figure 5). The data illustrate that nonhydrolyzable structural analogues such as 2′-OMe-NTPs, 5-substituted pyrimidine NTPs, and O^6-Me-GTP are the most potent inhibitors of DNA binding, despite the fact that their parent molecules, UTP and ATP, are good substrates for RecA NTPase activity. In contrast, those NTPs that can serve as substrates for DNA-dependent RecA hydrolysis do not facilitate extensive filament dissociation despite the fact that they are converted to the corresponding NDP during the experiment. In this context, it is important to distinguish between these NTPs that are

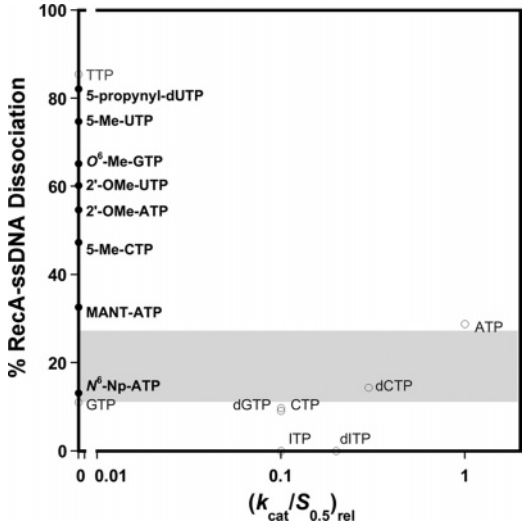

FIGURE 5: Analysis of the potential correlation between a NTP's ability to serve as a substrate for RecA-catalyzed hydrolysis and its ability to induce RecA−ssDNA filament dissociation. For each NTP, the relative NPF dissociation induced by 100 μM nucleotide was plotted as a function of the value of the relative specificity constant ($k_{cat}/S_{0.5}$) for that nucleotide. The k_{cat} and $S_{0.5}$ values were taken from Table 1. The relative NPF dissociation values are the mean of at least three independent experiments and were calculated by dividing the RecA concentration observed in the assay supernatant by the average of the maximum RecA concentration observed in the supernatant in three experiments. The data points for the canonical (r,d)NTPs are shown as empty circles, and those for the NTP analogues are shown as filled circles. For reference, the light gray box represents the NPF dissociation caused by 100 μM ADP ($21 \pm 6\%$).

not efficiently hydrolyzed and the classic nonhydrolyzable ATP analogues with phosphate isosteres. Members of the latter group, which includes ATPγS, ADP·AlF_4^-, and AMP-PNP, bind and stabilize the active NPF (*24*, *47*, *48*) and prevent ATP hydrolysis by simple competition (*48*). On the other hand, the NTP analogues evaluated in this paper bear substituents on the heterocycle or ribose moieties that prevent them from binding or stabilizing RecA in the active NPF conformation. We conclude that there is an apparent dichotomy between those NTPs that bind the active NPF and those that bind the inactive NPF and induce filament dissociation.

DISCUSSION

We have probed the specificity of the DNA-dependent NTP hydrolysis activity of RecA using a ligand-based approach involving a total of 28 prospective substrates comprising both canonical NTPs and synthetic analogues thereof. The kinetic parameters k_{cat} and $S_{0.5}$ were measured for each NTP. Those NTPs that were not subject to hydrolysis by RecA were then characterized with regard to their abilities to bind RecA nucleoprotein filaments in their active and inactive conformational states. The principle conclusion of this work is that the NTPs can be readily segregated into two groups based on mutually exclusive activities in three assays: (1) NTPs that preferentially bind the active NPF conformation and either serve as substrates for or competitively inhibit hydrolysis and (2) nonsubstrate NTPs that preferentially bind the inactive RecA conformation and facilitate RecA−ssDNA dissociation (Figure 6).

NTPs Are Conformationally Selective in Their Binding to RecA. Nineteen of the 28 tested NTPs served as substrates for RecA-catalyzed ATP hydrolysis. The NTPs' abilities as substrates were attenuated when certain structural features were present. Importantly, those same functional groups *enhanced* the NPF dissociative activities of the NTPs. The particular structural modifications included a 2′-*O*-methyl group on either a pyrimidine or a purine, substitution at the C5 position of a pyrimidine with a methyl or larger functional group, and naphthyl substituents at the N^6 position of a purine (Figure 2). Clearly, these key nucleotide functional groups, in combination with those of specific residues in the RecA protein, provide the molecular basis for the dichotomy between those NTPs that bind the active NPF and those that bind the inactive NPF.

The generality of the separation of NTPs into two groups of conformation-specific binders is supported by two observations. First, those NTPs that caused dissociation of RecA from DNA in the inactive conformation binding screen did not make for very potent inhibitors of RecA ATPase activity in vitro. In quantitative terms, the K_{ic} values measured for five nonsubstrate NTPs were at least 3-fold higher than the corresponding K_d^{app} values (data not shown). The data for MANT-ATP provide a second rationale for the distinction between those NTPs that bound the active and inactive conformations of RecA. Specifically, although MANT-ATP is not a substrate for hydrolysis by RecA, the nucleotide is a potent competitive inhibitor of RecA's ATPase activity but does not effectively induce NPF dissociation. In other words, MANT-ATP can be represented by the cartoon depicted in Figure 6B. This suggests that MANT-ATP is a high-affinity binder of the active NPF but a low-affinity binder of the inactive NPF. We conclude that the binding to RecA by NTPs is conformationally selective. This has important implications as discussed below.

Structual Basis for Conformationally Selective RecA Binding by NTPs. The available high-resolution structures of the *E. coli* RecA filament with nucleotide bound at the ATP binding site depict the inactive filament (*33*, *34*). As part of a recent comparative analysis of the RecA crystal structures with those of related ATP-dependent enzymes (*9*), we noted that the adenosine moiety in the RecA structures is located in a wide crevice near the surface of the protein (Figure 7A,C). The binding site is superficial and accessible, apparently providing room for a variety of voluminous substitutions on both the base and ribose moieties of a nucleotide. Consistent with this observation, the inactive RecA conformation accommodates many different nucleotides. With the exception of TTP and TDP, all of the canonical nucleoside di- and triphosphates, both ribo- and 2′-deoxyribonucleotides, induced similar extents of dissociation of RecA from ssDNA (Figure 4). Furthermore, several of the nonsubstrate nucleotide triphosphate analogues induced dissociation of between 30 and 90% of the DNA-bound RecA (Figure 5). This extent of NPF dissociation is equivalent to a maximum range in the apparent dissociation constants (K_d^{app}) between 10 and 250 μM. This rather modest range corroborates the expectation that the ATP binding site of RecA in its inactive conformation is not particularly selective.

In contrast to the observations with the inactive conformation of RecA, the active nucleoprotein filament has a more narrow tolerance for modified NTPs (Table 1). As a corollary

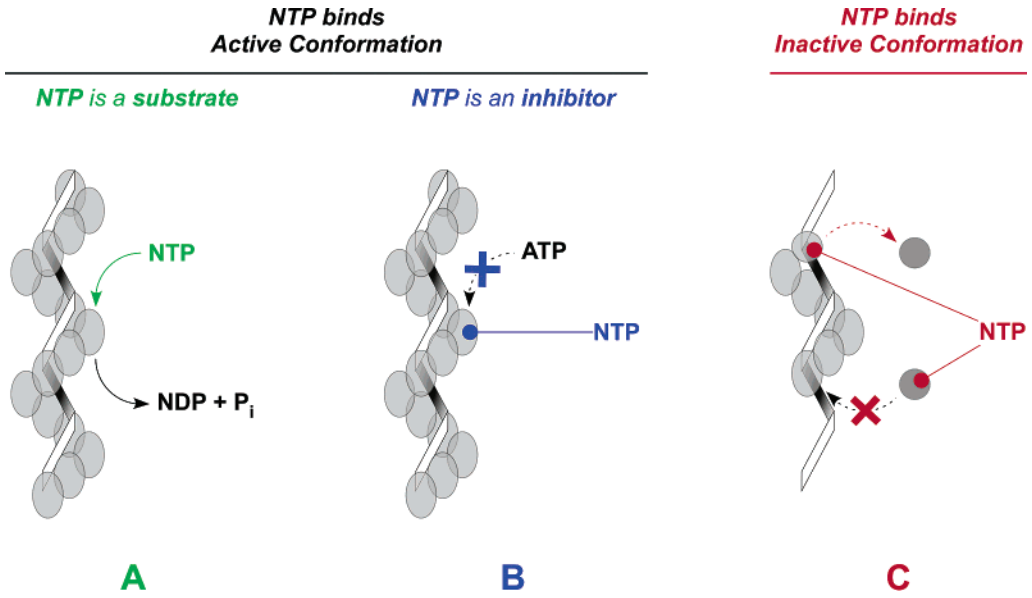

FIGURE 6: Summary of three different in vitro assays characterizing the binding of 28 NTPs to the two conformational states of the RecA nucleoprotein filament. The cartoons represent ssDNA (white ribbon) and either bound (light gray ovals) or free (dark gray circles) RecA protein monomers. A NTP binding the active nucleoprotein filament can either (A) be hydrolyzed by RecA or (B) competitively inhibit ATP hydrolysis. (C) A NTP which binds to and stabilizes the inactive conformation will cause the dissociation of RecA and ssDNA.

to the conclusion drawn above, a wide, solvent-accessible ATP binding cleft is not consistent with the high degree of selectivity noted for the active RecA conformation in our studies. The differences we observe in binding between the active and inactive conformations of RecA cannot be rationalized using the existing high-resolution crystal structures and require a different model for the conformation of the active RecA nucleoprotein filament.

The groups of Egelman and Campbell recently reported an 18 Å EM reconstruction of the extended NPF from which they developed a pseudoatomic model of the active state of RecA (*11*). A remarkable feature of the model is the reorientation of RecA monomers with respect to their crystallographic locations such that the ATP binding site is now located between adjacent monomers and comprises highly conserved residues on both subunits. Many important aspects of the model, including the location of the ATP site at the subunit interface, have been substantiated by analyses of the crystal structures of RecA homologues in extended filaments (*24*, *33*, *49*). We reconstructed the model of VanLoock et al. using the reported C_α coordinates as a template for the 1.9 Å structure of RecA bound to Mg·ADP recently reported by Xing and Bell (*33*) (Figure 7).

The active filament structural model suggests that a complete nucleotide binding site in the active conformation should be viewed as being composed of a primary binding site, which contains the P-loop of one RecA subunit in a NPF, and a secondary site comprising the interacting residues of the neighboring RecA monomer. The residues that come into the proximity of the primary ATP binding site upon activation are Lys216, Arg222, Lys248, Lys250, Pro254, and Phe255. The changes in the positions of these residues can be appreciated by comparison of the active filament model (Figure 7B,D) with the inactive filament crystal structure (Figure 7A,C). In the inactive filament structure, the ATP binding site should readily accommodate substituents on the nucleotide (Figure 7B). However, addition of voluminous moieties on the nucleotide in the active filament (Figure 7D) would create the potential for steric clashes with the protein side chains that have moved into position to interact with the bound nucleotide.

Influence of N^6-Substituted Adenine on Conformational Selectivity. We have shown that RecA tolerated as substrates ATP analogues modified at the N^6 position with functional groups as large as benzyl and phenyl but that *N^6*-(1-naphthyl)-ATP preferentially bound the inactive RecA conformation and induced dissociation. The structural model of VanLoock et al. for the active filament reveals several features that may rationalize the efficiency with which RecA is activated or deactivated by nucleotides modified at the N^6 position.

The *N^6*-phenyl-ATP analogue was hydrolyzed with kinetic parameters (k_{cat} = 23.5 min^{-1}, $S_{0.5}$ = 49 μM) nearly identical to those of ATP, the usual substrate for RecA. The larger, and presumably less constrained, benzyl group diminished the apparent affinity of the active NPF for the nucleotide almost 6-fold ($S_{0.5}$ = 281 μM) compared to that with ATP, but it increased the k_{cat} parameter by a surprising 65%. The fact that the small increase in size from phenyl to benzyl had a substantial influence on hydrolysis kinetic parameters was corroborated by the results with *N^6*-(1-naphthyl)-ATP. In this case, the larger naphthyl substituent at the N^6 position resulted in a nucleotide which could not be hydrolyzed by RecA at the concentrations that were tested. However, *N^6*-(1-naphthyl)-ATP bound the inactive RecA conformation and induced the dissociation of RecA from ssDNA.

In contrast to the inactive RecA conformation, which we have shown can uniquely accommodate a sterically demanding substituent at N^6 of ADP (*9*), the model of the active NPF predicts that the ATP binding site envelops the adenine moiety in a pocket and maintains close contact with its edge and both faces. Hence, it is reasonable to speculate that the residues from the secondary monomer are positioned close to the N^6 position of the bound nucleotide (Figure 7D). The smaller, more flexible substitutions such as phenyl and benzyl groups may not interfere, but as the size of the substitution

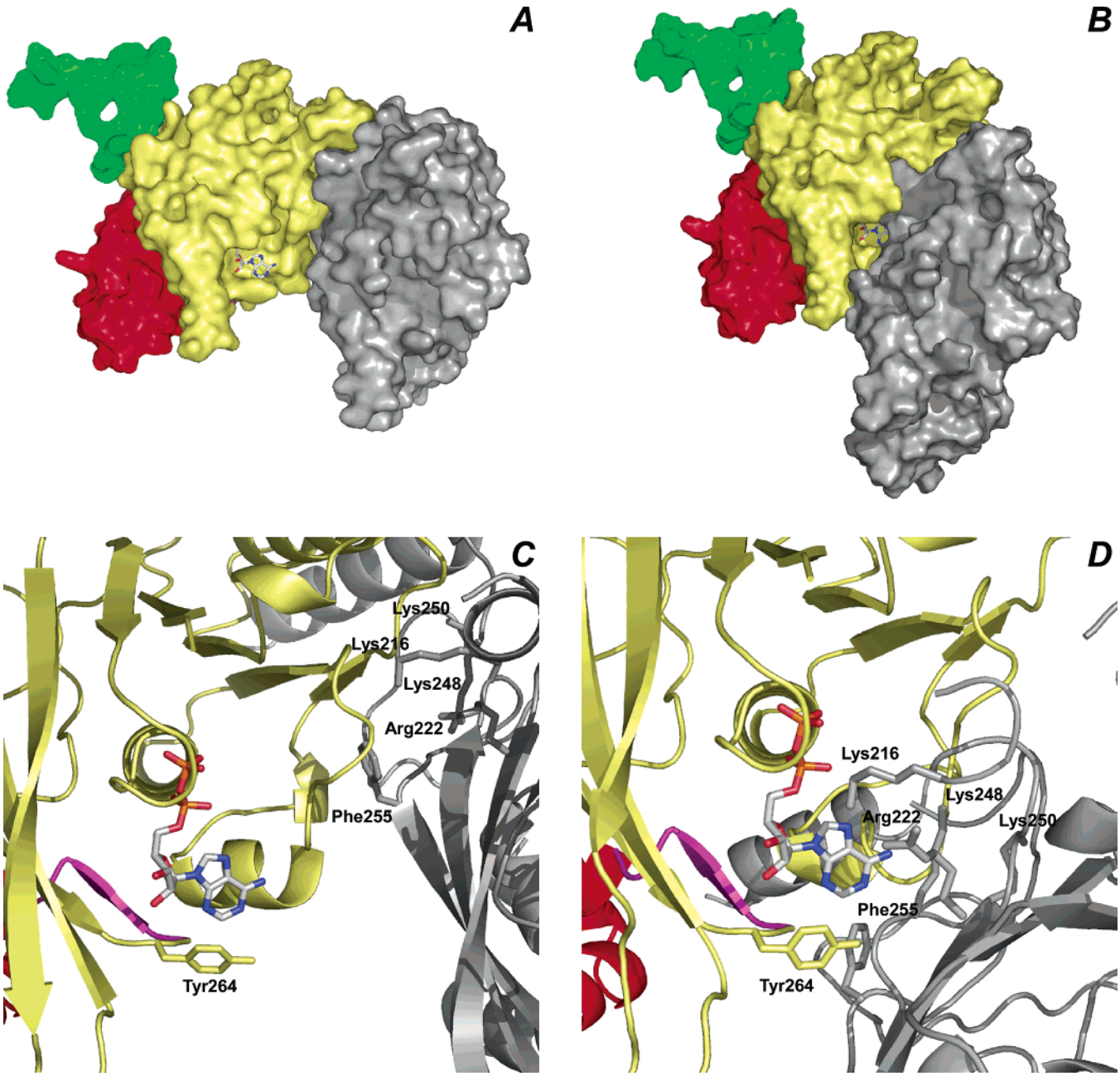

FIGURE 7: Structural models of the RecA ATP binding site in the inactive (A and C) and active (B and D) filament conformations of Asp100 and Arg100 with adjacent RecA monomers during filament assembly. Each panel depicts a RecA dimer wherein one subunit is colored according to its domain structure and the second monomer is gray. The domain coloring is as follows: N-terminal domain (residues 1−33) in green, core/ATP-binding domain (residues 34−260) in yellow, C-terminal domain (residues 271−323) in red, and the tether between the core and C-terminal domains (residues 261−270) in magenta. (A) RecA dimer from the crystal structure of the inactive filament state (*33*). The proteins are rendered as their Connolly surfaces, and the bound ADP molecule is rendered as a stick model. (B) RecA dimer from the VanLoock et al. structural model of the active filament state, rendered as in panel A. (C) Enhanced view of an ATP binding site from the crystal structure of the inactive filament state. The proteins are rendered as ribbon cartoons. The individual residues involved in interactions with the bound nucleotide are shown as stick models and labeled (see the text for details). (D) Enhanced view of an ATP binding site from the VanLoock et al. structural model of the active filament state, rendered as in panel C.

increases to that of the naphthyl group, there is the potential for steric clashes between the naphthyl group and the side chains of the secondary RecA monomer that have folded down to complete the binding pocket. We conclude that our observations regarding the influence of N^6-substituted adenine on the conformational selectivity of NTP binding are fully consistent with the VanLoock et al. model for the active filament.

Influence of 2′-O-Substituted Ribose on Conformational Selectivity. We have shown that RecA activity is exquisitely sensitive to modifications at the ribose 2′ position of the NTPs. The fact that dATP has been demonstrated to be a better substrate for RecA ATPase than ATP (*50*) indicates that the presence of a hydroxyl group at the 2′ position is not necessary to achieve the activated conformation of the RecA NPF. Our own data show that, although hydrogen, hydroxyl, fluorine, or amine substituents are well tolerated at the 2′ position, steric occlusion by functionalities as large or larger than a methoxy group abrogated the ability of a NTP to serve as a substrate for RecA NTP hydrolysis.

Interestingly, while 2′-OMe-ATP selectively binds the inactive RecA conformation, substitution with an aromatic group at the 2′ position makes for a NTP that does not bind the inactive conformation but is a sub-micromolar inhibitor of RecA's ATPase activity.

In the crystal structures of RecA bound to nucleotides, the residue which appears to be closest to the 2′-OH of the ribose moiety is Tyr264 (*33*, *34*). This residue is highly conserved (*6*), and mutational analysis has shown it to be crucial for proper RecA function (*51*, *52*). Tyr264 lies within a loop that connects the core domain of RecA, which includes the ATP binding site, with the RecA C-terminal domain (residues 270−352; Figure 7). The C-terminal domain of RecA is postulated to regulate RecA activity by acting as a switch to modulate DNA binding and the subsequent hydrolysis of ATP (*34*, *53*−*55*). The EM reconstructions directly demonstrated that the state of the bound nucleotide modulates the structure of the C-terminal domain, and Egelman and co-workers speculated that allosteric coupling between these two substructures may be communicated in both directions (*11*). The Tyr264-containing region, which tethers the core and C-terminal domains, may provide a means of transmitting allosteric information between the ATP binding site and the C-terminal domain (*24*). We propose that steric interference with the Tyr264 residue is the key molecular determinant of the inability of RecA to hydrolyze NTPs modified at the ribose 2′ position with functional groups as large or larger than an *O*-methyl group. The steric occlusion generated by such analogues could prevent the internal degrees of rotational freedom required by Tyr264 in this tether region that facilitates the rearrangement of the C-terminus in space. In turn, the restrictions on internal rearrangements would preclude the formation of the active conformation of RecA.

The inhibition of ATPase activity we observe with MANT-ATP can be rationalized by interactions between the additional ribose 2′(3′)-*O*-anthraniloyl moiety and the Tyr264 side chain. We speculate that π-stacking interactions between an aromatic group at the 2′ position of a nucleotide analogue and the phenol side chain of Tyr264 may enhance the affinity of the nucleotide analogue for the active NPF, allowing it to more effectively compete with ATP for the nucleotide binding site. When RecA is in the inactive conformation, the same aromatic substituent on the nucleotide analogue may be sterically occluded from the ATP binding site such that the nucleotide analogue binds with only low affinity. Experiments are underway to test this structural hypothesis.

CONCLUSION

In summary, we have probed the nucleotide binding site of the RecA protein using a total of 28 prospective ligands comprising both canonical NTPs and 19 synthetic analogues never previously tested with RecA. We reported an assay to determine whether a given nucleotide analogue can bind to and stabilize the inactive conformation of RecA, and we have also shown that RecA ATPase activity can be significantly inhibited in vitro using substituted analogues of nucleotide triphosphates. Our results clearly demonstrate that the ATP binding site of RecA is exquisitely sensitive to some modifications at certain positions on nucleotides yet surprisingly tolerant to others. Indeed, the NTPs can be readily segregated into two groups based on three activity assays: (1) NTPs that preferentially bind the active NPF conformation and either serve as substrates for or competitively inhibit hydrolysis and (2) nonsubstrate NTPs that preferentially bind the inactive RecA conformation and facilitate RecA−ssDNA dissociation (Figure 6). The observed trends are consistent with the structural model of the active NPF proposed by Egelman, Campbell, and their co-workers. Our systematic, ligand-based approach provides insight into differences between the ATP binding site of RecA in its inactive conformation and the ATP binding site of the active nucleoprotein filament. We therefore think these insights will enhance our understanding of the conformational selectivity of RecA−ligand interactions and provide information for the refinement of pseudoatomic models of the active conformation of the RecA filament. Moreover, our laboratory is using these insights for the design of bioorthogonal RecA-NTP pairs for future chemical biology experiments and for the development of lead compounds for inhibiting RecA-dependent processes in vivo.

REFERENCES

1. Matic, I., Taddei, F., and Radman, M. (2004) Survival versus maintenance of genetic stability: A conflict of priorities during stress, *Res. Microbiol. 155*, 337−41.
2. Hersh, M. N., Ponder, R. G., Hastings, P. J., and Rosenberg, S. M. (2004) Adaptive mutation and amplification in *Escherichia coli*: Two pathways of genome adaptation under stress, *Res. Microbiol. 155*, 352−9.
3. Foster, P. L. (2005) Stress responses and genetic variation in bacteria, *Mutat. Res. 569*, 3−11.
4. Beaber, J. W., Hochhut, B., and Waldor, M. K. (2004) SOS response promotes horizontal dissemination of antibiotic resistance genes, *Nature 427*, 72−4.
5. Hastings, P. J., Rosenberg, S. M., and Slack, A. (2004) Antibiotic-induced lateral transfer of antibiotic resistance, *Trends Microbiol. 12*, 401−4.
6. Roca, A. I., and Cox, M. M. (1997) RecA protein: Structure, function, and role in recombinational DNA repair, *Prog. Nucleic Acid Res. Mol. Biol. 56*, 129−223.
7. Kowalczykowski, S. C., and Eggleston, A. K. (1994) Homologous pairing and DNA strand-exchange proteins, *Annu. Rev. Biochem. 63*, 991−1043.
8. Lee, A. M., and Singleton, S. F. (2004) Inhibition of the *Escherichia coli* RecA protein: Zinc(II), copper(II) and mercury(II) trap RecA as inactive aggregates, *J. Inorg. Biochem. 98*, 1981−6.
9. Lee, A. M., Ross, C. T., Zeng, B. B., and Singleton, S. F. (2005) A Molecular Target for Suppression of the Evolution of Antibiotic Resistance: Inhibition of the *Escherichia coli* RecA Protein by N^6-(1-Naphthyl)-ADP, *J. Med. Chem. 48*, 5408−11.
10. Nishinaka, T., Ito, Y., Yokoyama, S., and Shibata, T. (1997) An extended DNA structure through deoxyribose-base stacking induced by RecA protein, *Proc. Natl. Acad. Sci. U.S.A. 94*, 6623−8.
11. VanLoock, M. S., Yu, X., Yang, S., Lai, A. L., Low, C., Campbell, M. J., and Egelman, E. H. (2003) ATP-mediated conformational changes in the RecA filament, *Structure 11*, 187−96.
12. Yamazaki, J., Horii, T., Sekiguchi, M., and Takahashi, M. (2003) Regulation of RecA protein binding to DNA by opposing effects of ATP and ADP on inter-domain contacts: Analysis by urea-induced unfolding of wild-type and C-terminal truncated RecA, *J. Mol. Biol. 329*, 363−70.
13. Ellouze, C., Selmane, T., Kim, H. K., Tuite, E., Norden, B., Mortensen, K., and Takahashi, M. (1999) Difference between active and inactive nucleotide cofactors in the effect on the DNA binding and the helical structure of RecA filament dissociation of RecA−DNA complex by inactive nucleotides, *Eur. J. Biochem. 262*, 88−94.
14. Yu, X., and Egelman, E. H. (1990) Image analysis reveals that *Escherichia coli* RecA protein consists of two domains, *Biophys. J. 57*, 555−66.

15. Lee, J. W., and Cox, M. M. (1990) Inhibition of recA protein promoted ATP hydrolysis. 2. Longitudinal assembly and disassembly of recA protein filaments mediated by ATP and ADP, *Biochemistry 29*, 7677−83.
16. Roca, A. I., and Singleton, S. F. (2003) Direct evaluation of a mechanism for activation of the RecA nucleoprotein filament, *J. Am. Chem. Soc. 125*, 15366−75.
17. Weinstock, G. M., McEntee, K., and Lehman, I. R. (1981) Hydrolysis of nucleoside triphosphates catalyzed by the recA protein of *Escherichia coli*. Characterization of ATP hydrolysis, *J. Biol. Chem. 256*, 8829−34.
18. Weinstock, G. M., and McEntee, K. (1981) RecA protein-dependent proteolysis of bacteriophage lambda repressor. Characterization of the reaction and stimulation by DNA-binding proteins, *J. Biol. Chem. 256*, 10883−8.
19. Menge, K. L., and Bryant, F. R. (1992) Effect of nucleotide cofactor structure on recA protein-promoted DNA pairing. 2. DNA renaturation reaction, *Biochemistry 31*, 5158−65.
20. Menge, K. L., and Bryant, F. R. (1992) Effect of nucleotide cofactor structure on recA protein-promoted DNA pairing. 1. Three-strand exchange reaction, *Biochemistry 31*, 5151−7.
21. Konola, J. T., Nastri, H. G., Logan, K. M., and Knight, K. L. (1995) Mutations at Pro67 in the RecA protein P-loop motif differentially modify coprotease function and separate coprotease from recombination activities, *J. Biol. Chem. 270*, 8411−9.
22. Stole, E., and Bryant, F. R. (1995) Spectroscopic demonstration of a linkage between the kinetics of NTP hydrolysis and the conformational state of the recA-single-stranded DNA complex, *J. Biol. Chem. 270*, 20322−8.
23. McGrew, D. A., and Knight, K. L. (2003) Molecular design and functional organization of the RecA protein, *Crit. Rev. Biochem. Mol. Biol. 38*, 385−432.
24. Bell, C. E. (2005) Structure and mechanism of *Escherichia coli* RecA ATPase, *Mol. Microbiol. 58*, 358−66.
25. Katz, F. S., and Bryant, F. R. (2003) Three-strand exchange by the *Escherichia coli* RecA protein using ITP as a nucleotide cofactor: Mechanistic parallels with the ATP-dependent reaction of the RecA protein from *Streptococcus pneumoniae*, *J. Biol. Chem. 278*, 35889−96.
26. Singleton, S. F., Simonette, R. A., Sharma, N. C., and Roca, A. I. (2002) Intein-mediated affinity-fusion purification of the *Escherichia coli* RecA protein, *Protein Expression Purif. 26*, 476−88.
27. Craig, N. L., and Roberts, J. W. (1981) Function of nucleoside triphosphate and polynucleotide in *Escherichia coli* recA protein-directed cleavage of phage lambda repressor, *J. Biol. Chem. 256*, 8039−44.
28. Webb, M. R., and Hunter, J. L. (1992) Interaction of GTPase-activating protein with p21ras, measured using a continuous assay for inorganic phosphate release, *Biochem. J. 287* (Part 2), 555−9.
29. Neet, K. E. (1980) Cooperativity in enzyme function: Equilibrium and kinetic aspects, *Methods Enzymol. 64*, 139−92.
30. Menge, K. L., and Bryant, F. R. (1988) ATP-stimulated hydrolysis of GTP by RecA protein: Kinetic consequences of cooperative RecA protein-ATP interactions, *Biochemistry 27*, 2635−40.
31. Berger, M. D., Lee, A. M., Simonette, R. A., Jackson, B. E., Roca, A. I., and Singleton, S. F. (2001) Design and evaluation of a tryptophanless RecA protein with wild-type activity, *Biochem. Biophys. Res. Commun. 286*, 1195−203.
32. Morrical, S. W., Lee, J., and Cox, M. M. (1986) Continuous association of *Escherichia coli* single-stranded DNA binding protein with stable complexes of recA protein and single-stranded DNA, *Biochemistry 25*, 1482−94.
33. Xing, X., and Bell, C. E. (2004) Crystal structures of *Escherichia coli* RecA in complex with MgADP and MnAMP-PNP, *Biochemistry 43*, 16142−52.
34. Story, R. M., and Steitz, T. A. (1992) Structure of the recA protein-ADP complex, *Nature 355*, 374−6.
35. Xing, X., and Bell, C. E. (2004) Crystal structures of *Escherichia coli* RecA in a compressed helical filament, *J. Mol. Biol. 342*, 1471−85.
36. Yamagata, Y., Kohda, K., and Tomita, K. (1988) Structural studies of O6-methyldeoxyguanosine and related compounds: A promutagenic DNA lesion by methylating carcinogens, *Nucleic Acids Res. 16*, 9307−21.
37. Tavale, S. S., and Sobell, H. M. (1970) Crystal and molecular structure of 8-bromoguanosine and 8-bromoadenosine, two purine nucleosides in the syn conformation, *J. Mol. Biol. 48*, 109−23.
38. Ikehara, M., Uesugi, S., and Yoshida, K. (1972) Conformation of purine nucleoside pyrophophates as studied by circular dichroism, *Biochemistry 11*, 836−42.
39. Defais, M., Phez, E., and Johnson, N. P. (2003) Kinetic mechanism for the formation of the presynaptic complex of the bacterial recombinase RecA, *J. Biol. Chem. 278*, 3545−51.
40. Paulus, B. F., and Bryant, F. R. (1997) Time-dependent inhibition of recA protein-catalyzed ATP hydrolysis by ATPγS: Evidence for a rate-determining isomerization of the recA-ssDNA complex, *Biochemistry 36*, 7832−8.
41. Weinstock, G. M., McEntee, K., and Lehman, I. R. (1981) Hydrolysis of nucleoside triphosphates catalyzed by the recA protein of *Escherichia coli*. Hydrolysis of UTP, *J. Biol. Chem. 256*, 8856−8.
42. Weinstock, G. M., McEntee, K., and Lehman, I. R. (1981) Hydrolysis of nucleoside triphosphates catalyzed by the recA protein of *Escherichia coli*. Steady-state kinetic analysis of ATP hydrolysis, *J. Biol. Chem. 256*, 8845−9.
43. Lee, J. W., and Cox, M. M. (1990) Inhibition of recA protein promoted ATP hydrolysis. 1. ATPγS and ADP are antagonistic inhibitors, *Biochemistry 29*, 7666−76.
44. Karasaki, Y., and Higashi, K. (1984) Inhibition of ATPase activity of the recA protein by ATP ribose-modified analogs, *Arch. Biochem. Biophys. 233*, 796−9.
45. Lee, A. M., Ross, C. T., Zeng, B. B., and Singleton, S. F. (2005) A Molecular Target for Suppression of the Evolution of Antibiotic Resistance: Inhibition of the *Escherichia coli* RecA Protein by N^6-(1-Naphthyl)-ADP, *J. Med. Chem. 48*, 5408−11.
46. Menetski, J. P., and Kowalczykowski, S. C. (1985) Interaction of recA protein with single-stranded DNA. Quantitative aspects of binding affinity modulation by nucleotide cofactors, *J. Mol. Biol. 181*, 281−95.
47. Weinstock, G. M., McEntee, K., and Lehman, I. R. (1981) Interaction of the recA protein of *Escherichia coli* with adenosine 5′-O-(3-thiotriphosphate), *J. Biol. Chem. 256*, 8850−5.
48. Moreau, P. L., and Carlier, M. F. (1989) RecA protein-promoted cleavage of LexA repressor in the presence of ADP and structural analogues of inorganic phosphate, the fluoride complexes of aluminum and beryllium, *J. Biol. Chem. 264*, 2302−6.
49. Wu, Y., He, Y., Moya, I. A., Qian, X., and Luo, Y. (2004) Crystal structure of archaeal recombinase RADA: A snapshot of its extended conformation, *Mol. Cell 15*, 423−35.
50. Katz, F. S., and Bryant, F. R. (2001) Interdependence of the kinetics of NTP hydrolysis and the stability of the RecA-ssDNA complex, *Biochemistry 40*, 11082−9.
51. Freitag, N. E., and McEntee, K. (1991) Site-directed mutagenesis of the RecA protein of *Escherichia coli*. Tyrosine 264 is required for efficient ATP hydrolysis and strand exchange but not for LexA repressor inactivation, *J. Biol. Chem. 266*, 7058−66.
52. Eriksson, S., Norden, B., Morimatsu, K., Horii, T., and Takahashi, M. (1993) Role of tyrosine residue 264 of RecA for the binding of cofactor and DNA, *J. Biol. Chem. 268*, 1811−6.
53. Eggler, A. L., Lusetti, S. L., and Cox, M. M. (2003) The C terminus of the *Escherichia coli* RecA protein modulates the DNA binding competition with single-stranded DNA-binding protein, *J. Biol. Chem. 278*, 16389−96.
54. Kurumizaka, H., Aihara, H., Ikawa, S., Kashima, T., Bazemore, L. R., Kawasaki, K., Sarai, A., Radding, C. M., and Shibata, T. (1996) A possible role of the C-terminal domain of the RecA protein. A gateway model for double-stranded DNA binding, *J. Biol. Chem. 271*, 33515−24.
55. Lusetti, S. L., Shaw, J. J., and Cox, M. M. (2003) Magnesium ion-dependent activation of the RecA protein involves the C terminus, *J. Biol. Chem. 278*, 16381−8.

BI052298H